HHS Public Access

Author manuscript

Nat Neurosci. Author manuscript; available in PMC 2017 March 28.

Published in final edited form as:

Nat Neurosci. 2014 September ; 17(9): 1190–1197. doi:10.1038/nn.3772.

LKB1 and AMPK regulate synaptic remodeling in old age

Melanie A Samuel[1,8], **P Emanuela Voinescu**[1,8], **Brendan N Lilley**[1], **Rafa de Cabo**[2], **Marc Foretz**[3,4,5], **Benoit Viollet**[3,4,5], **Basil Pawlyk**[6], **Michael A Sandberg**[6], **Demetrios G Vavvas**[7], and **Joshua R Sanes**[1]

[1]Department of Molecular and Cellular Biology and Center for Brain Science, Harvard University, Cambridge, Massachusetts, USA

[2]Laboratory of Experimental Gerontology, Translational Gerontology Branch, Intramural Research Program, National Institute on Aging, Baltimore, Maryland, USA

[3]Inserm, U1016, Institut Cochin, Paris, France

[4]CNRS, UMR8104, Paris, France

[5]Université Paris Descartes, Sorbonne Paris Cité, Paris, France

[6]The Berman-Gund Laboratory for the Study of Retinal Degenerations, Department of Ophthalmology, Massachusetts Eye and Ear Infirmary, Harvard Medical School, Boston, Massachusetts, USA

[7]Retina Service, Angiogenesis Laboratory, Massachusetts Eye and Ear Infirmary, Department of Ophthalmology, Harvard Medical School, Boston, Massachusetts, USA

Abstract

Age-related decreases in neural function result in part from alterations in synapses. To identify molecular defects that lead to such changes, we focused on the outer retina, in which synapses are markedly altered in old rodents and humans. We found that the serine/threonine kinase LKB1 and one of its substrates, AMPK, regulate this process. In old mice, synaptic remodeling was accompanied by specific decreases in the levels of total LKB1 and active (phosphorylated) AMPK. In the absence of either kinase, young adult mice developed retinal defects similar to those that occurred in old wild-type animals. LKB1 and AMPK function in rod photoreceptors where their loss leads to aberrant axonal retraction, the extension of postsynaptic dendrites and the formation of ectopic synapses. Conversely, increasing AMPK activity genetically or pharmacologically attenuates and may reverse age-related synaptic alterations. Together, these results identify molecular determinants of age-related synaptic remodeling and suggest strategies for attenuating these changes.

The nervous system changes in many ways as we age: sensory, motor and cognitive functions decrease, and the risk of neurodegenerative disease increases[1]. Although multiple factors likely contribute to age-associated changes in the nervous system, several lines of evidence suggest that defects in synapses have a central role[2]. Synapses are especially

Correspondence should be addressed to J.R.S. (sanesj@mcb.harvard.edu).

[8]These authors contributed equally to this work.

vulnerable to damage as a result of their distance from the cell body, high complexity and extensive regulation. In addition, age-related synaptic dysfunction is thought to precipitate neurological degeneration in age-related diseases[3,4]. However, the molecular alterations that underlie age-related synaptic changes remain unknown[2].

A major difficulty in deciphering these molecular causes is that most documented age-related alterations in synaptic structure, function and number are subtle or difficult to quantify[1,2]. To circumvent this problem, we focused on synapses in the outer retina, which are particularly large and undergo marked age-related alterations in rodents and humans[5–8]. In the outer retina, two types of photoreceptors, rods and cones, form synapses with two types of interneurons, bipolar and horizontal cells[9,10]. In young adults, these synapses localize to a narrow band known as the outer plexiform layer (OPL), where photoreceptor and interneuron processes terminate (Fig. 1a). In old retina, aberrant horizontal and bipolar neuron processes sprout far beyond the OPL into the photoreceptor nuclear layer, where they form numerous ectopic synapses. These changes provide a robust structural biomarker that we used to assay candidate mediators of synaptic aging.

One promising candidate is the serine/theonine kinase LKB1 (also known as *Stk11*). LKB1 is a multifunctional enzyme that regulates cellular energy homeostasis, cell proliferation, polarity and axon outgrowth by activating kinases of the AMPK subfamily, including AMPK itself[11–14]. In addition, LKB1 and AMPK have been shown to modulate longevity[15–17] and have been implicated in age-related diseases, including Alzheimer's disease and cancer[18,19]. We found that LKB1 and AMPK contribute to the regulation of synaptic aging. Old age specifically decreased the activity of the LKB1-AMPK axis in retina. Inactivating either LKB1 or AMPK accelerated synaptic aging, whereas activating this signaling pathway genetically or pharmacologically suppressed the pathological changes in old animals. Finally, we used single neuron visualization approaches to uncover the cellular basis of synaptic aging and found that rod axon retraction is a key driver. Together, these results identify the LKB1-AMPK pathway as a molecular determinant of age-related synaptic remodeling and suggest approaches for attenuating this process.

RESULTS

Deletion of *LKB1* induces age-related changes in young mice

Given that *Lkb1* null mice die during embryogenesis, we used a conditional allele ($Lkb1^{F/F}$)[20] that is specifically deleted from retinal progenitors when paired with *Six3-Cre*, *Chx10-Cre* or *Pax6-Cre*; the resulting mice are referred to as $Lkb1^{ret}$. Young adult $Lkb1^{ret}$ mice bore numerous horizontal and bipolar cell sprouts that resembled those of old (24–28 month old) wild-type animals (Fig. 1b–d). Based on this similarity, we compared old wild-type and young $Lkb1^{ret}$ mice in detail.

$Lkb1^{ret}$ retinas developed normally, but, by 1 month of age, sprouts in $Lkb1^{ret}$ mice were similar in structure, number and length to those in old wild-type mice. (Fig. 1e,f and Supplementary Fig. 1). Moreover, in both old wild-type and young $Lkb1^{ret}$ mice, horizontal and bipolar cell sprouts cofasciculated (Supplementary Fig. 2a,b) and the OPL thinned and contained displaced nuclei (Fig. 1g and Supplementary Fig. 2c,d). Staining with synaptic

markers revealed that sprouts in *Lkb1*^{ret} and old animals were dotted with numerous ectopic synapses bearing both pre- and postsynaptic proteins (Fig. 1h and Supplementary Fig. 3). Electron microscopy revealed that the ectopic synapses displayed the triad structure and ribbon typical of rod spherule synapses in the OPL of young animals (Fig. 1i). Although the number of ectopic synapses increased ~40-fold (see below), the remodeling involved more than a shift in synaptic position, as the total number of synapses decreased by ~20% in both old and *Lkb1*^{ret} outer retina (36.7 ± 4.4 synapses per 100 μm in young controls versus 28.4 ± 4.3 and 30.9 ± 4.3 in *Lkb1*^{ret} and old mice, respectively; mean ± s.d., $P < 0.0001$). Control (*Lkb1*$^{F/F}$) retinas exhibited proper retinal organization (Fig. 1b), as did heterozygotes (*Lkb1*$^{F/+}$; *Six3-Cre* and *Lkb1*$^{F/+}$; *Chx10-Cre*), which retained normal levels of LKB1 despite having only a single copy of *Lkb1* (Supplementary Fig. 4).

We also recorded electroretinograms (ERGs) to determine whether young LKB1-deficient animals exhibit alterations in retinal function similar to those that have been reported for old wild-type mice[21]. The ERG a-wave represents electrical activity in photoreceptors, whereas the b-wave is derived from summed synaptic responses in both inner and outer retina. Responses in dark- and light-adapted retinas represent scotopic (rod-dominant) and photopic (cone- isolated) signals, respectively. Dark-adapted a- and b-wave amplitudes were significantly lower in *Lkb1*^{ret} animals than in controls (48% and 60% reduction, respectively; $P \leq 0.004$), indicating a defect in rod-mediated signaling. Light-adapted (cone) ERG b-waves were also reduced (Table 1 and Supplementary Fig. 5). Both defects resemble those observed in old mice[21] (B.P., unpublished data).

LKB1 is required in rods to maintain outer retina synapses

We next investigated the cellular basis of these structural alterations. In mice, rods comprise the majority of photoreceptors (97%) and have a high demand for energy as a result of the biochemistry that underlies visual transduction[22]. These features make them good candidates for driving LKB1-dependent remodeling. We selectively deleted *Lkb1* from rod photoreceptors using a transgenic line that expresses *Cre* only in these cells[23]. Deletion of *Lkb1* in rods alone (*Lkb1*^{rod}) induced sprouting of both rod bipolar and horizontal cells similar to that observed in whole retina deletion (Fig. 2a). Moreover, *Lkb1*^{rod} mice developed similar numbers of ectopic synapses as *Lkb1*^{ret} and aged animals (16.7 ± 6.2 versus 16.2 ± 6.3 ectopic synapses per 100 μm in *Lkb1*^{rod} and *Lkb1*^{ret}, respectively; Fig. 2b). However, sprouting was delayed in *Lkb1*^{rod} retinas by approximately 1 month compared with *Lkb1*^{ret} retinas (data not shown), suggesting that, although rods are the primary driver of remodeling, other cells may contribute.

We next sought to distinguish the function of LKB1 in development from its roles in synaptic maintenance. To this end, we used adeno-associated virus (AAV) 2/5 expressing Cre to delete *Lkb1* in adults. This serotype infected photoreceptors selectively (Supplementary Fig. 6), allowing for targeted gene manipulation. Deletion of *Lkb1* from adult photoreceptors caused sprouting similar to that observed in *Lkb1*^{rod} retinas (Fig. 2c), indicating that LKB1 is required for maintenance of normal synaptic architecture in the OPL.

LKB1 functions through AMPK to regulate synaptic aging

In view of the parallels between aged and *Lkb1*^{ret} animals, we next asked whether defects in LKB1 signaling might lead to age-related alterations. We considered three possibilities. First, LKB1 levels might decline in aged retina. Immunoblotting revealed that LKB1 levels decreased by ~20% in whole retina and isolated photoreceptors of old mice (Fig. 3a,b). This decrease was significant ($P \leq 0.004$) and might contribute to age-related synaptic alterations, but seems unlikely to account for them completely. Second, in the absence of LKB1, critical synaptic components might be downregulated or mislocalized. This possibility was suggested by reports that mutant mice lacking the photoreceptor nerve terminal proteins CACNA1f and Bassoon show OPL remodeling that is similar in some respects to that in old retina[24–27]. However, no significant change was observed in the level or synaptic localization of these or other synaptic proteins by immunoblotting or staining ($P \geq 0.7$; Figs. 1h and 3c,d, and Supplementary Fig. 3).

Finally, downstream components of the LKB1 signaling pathway might be compromised in aged retina. LKB1 phosphorylates 14 related serine/threonine kinases at a critical site in an activation loop; unless this site is phosphorylated, the kinases are catalytically inactive[11]. Of these kinases, at least eight are good candidate mediators of the LKB1 effect: SAD-A and SAD-B, MARK1–4, and AMPKα1/α2. All of these proteins regulate neuronal polarity and axon outgrowth[12,14,28–31], and AMPK is the primary target through which LKB1 regulates energy homeostasis[32]. *Sad*, *Mark*, *Ampk* and *Lkb1* are all expressed in retina[12] (Supplementary Fig. 7 and data not shown). We probed *Lkb1*-deficient and old retinas with antibodies specific for the phosphorylated activation loops of SAD, MARK or AMPK proteins. Deletion of *Lkb1* led to a ~75% decrease in the levels of phosphorylated SAD, MARK and AMPK (Fig. 3e,f). In old retina, however, the activation levels of all LKB1 targets were normal, with the exception of AMPK. Old age induced an ~80% decrease in AMPK phosphorylation (assayed with an antibody that recognizes both AMPKα1 and α2), although total AMPK protein levels were unchanged (Fig. 3e,g). Consistent with decreased levels of AMPK activity, the levels of phosphorylated acetyl-CoA carboxylase (pACC), an AMPK substrate[32] significantly declined in both old and LKB1-deficient retina ($P \leq 0.008$, Fig. 3e–g). The decrease in phosphorylated AMPK (pAMPK) in both LKB1-deficent and old retinas suggests that LKB1 acts through AMPK to maintain retinal synapses and that loss of pAMPK may underlie age-related synaptic remodeling.

Based on these results, we asked whether AMPK is required to maintain outer retinal synapses. To circumvent possible developmental affects, we used AAV2/5-Cre to inactivate both AMPK subunits in photoreceptors of adult *Ampkα1* and *Ampkα*2 (also known as *Prkaa1* and *Prkaa2*) conditional double mutants (*Ampkα1α2*$^{F/F}$). AMPK inactivation induced sprouting of rod bipolar and horizontal cells and formation of ectopic synapses (*Ampkα1α2*$^{F/F}$/AAV-Cre) at levels similar to those observed in LKB1 mutants and old animals (Fig. 4a–c). These results indicate that similar to LKB1, AMPK is required to prevent age-related outer retina remodeling.

We then asked whether AMPK functions downstream of LKB1. To this end, we generated AAV2/5 encoding a constitutively active form of AMPK (CA-AMPK)[33] and used it to infect photoreceptors in *Lkb1*^{rod} mice shortly after birth, before sprouts develop. CA-AMPK

reduced ectopic synapse formation in infected regions by ~35% (Fig. 4d,e). This value likely underestimates the efficacy of CA-AMPK, as not all photoreceptors were infected. Thus, restoring AMPK function in the absence of LKB1 can prevent age-related synaptic remodeling.

Finally, we tested the specificity of the LKB1-AMPK pathway in maintaining outer retina synapses using animals deficient for alternative signaling proteins. Given that SAD-A and SAD-B are required for axon formation in cortex downstream of LKB1 (ref. 12), we tested their role in outer retina using conditional SAD-A/SAD-B knockouts. Retinal development proceeded normally in these animals, and no ectopic synapses were observed (Supplementary Fig. 8a–c). We also asked whether an alternative AMPK-activating kinase, TAK1, might be involved in age-related synaptic remodeling. Animals deficient in retinal TAK1 showed no evidence of defects or alterations in outer retina organization (Supplementary Fig. 8d–f). Taken together, these results indicate that the LKB1-AMPK pathway specifically maintains synaptic localization.

Rod photoreceptor retraction drives synaptic remodeling

How might alterations in the LKB1-AMPK pathway in rods lead to alterations in horizontal and bipolar cells? To address this issue, we labeled individual photoreceptors using AAV2/5-GFP at low titer. We found that rod axons frequently retracted in young adult *Lkb1*^{ret}, *Lkb1*^{rod} and *Ampkα1α2*$^{F/F}$/AAV-Cre mutants and in old wild-type mice, but not in young adult wild-type controls (Fig. 5a and Supplementary Fig. 9). Rod bipolar and horizontal cells sprouted near the tips of these axons (Fig. 5b and data not shown). To establish an association between individual retracted rods and ectopic sprouts, we deleted either *Lkb1* or *Ampk* from isolated photoreceptors using AAV2/5-Cre at low titer. Sprouts formed directly below *Lkb1*- and *Ampk*-deficient cells (Fig. 5c,d). Moreover, sprouting was largely restricted to the postsynaptic partners of rods. Horizontal cells are polarized, with dendrites contacting cones and axons contacting rods, and these compartments are readily distinguished by their morphology[34] (Fig. 1a). In *Lkb1* mutants and old animals, axons of horizontal cells sprouted far more than dendrites (Fig. 5e), consistent with rod-driven remodeling. Likewise, although rod bipolars sprouted extensively, bipolar subtypes that selectively contact cones[35] sprouted rarely (Supplementary Fig. 10a).

To determine whether rod retraction could account for the level of ectopic synapse formation that we observed in young LKB1-deficient and old wild-type animals, we labeled photoreceptors more densely using AAV2/5-GFP (Fig. 6a). Sections were co-stained either with PSD-95 to mark rod spherule synaptic terminals[36] or with Bassoon to mark all photoreceptor synapses[37]. Quantification of OPL-restricted and ectopic GFP/PSD95 double-positive rod spherules revealed that ~50% of rod terminals were retracted in young LKB1-deficient and old wild-type animals (Fig. 6b). Similar results were obtained following Bassoon staining and quantification for total ectopic synapse formation (~48%; Fig. 6c). Thus, rod terminals retract frequently, and the percentage of retracted rods terminals is consistent with the percentage of ectopic synapses.

In mouse outer retina, rods outnumber cones 50:1. As a result, changes in large numbers of rods terminals might obscure cone synapse remodeling. To ask whether cone photoreceptors

retract, we labeled these neurons and their pedicle synapses with mouse cone arrestin. Retraction was rare (Supplementary Fig. 10b). We did observe subtle alterations in cone terminal structure in both old wild-type and young *Lkb1*^{ret} retinas (Supplementary Fig. 10c), although detailed analyses of these changes was beyond the resolution limit of confocal microscopy. This cellular specificity further emphasizes the parallel between age-related and LKB1/AMPK-dependent alterations and supports the idea that LKB1-AMPK–mediated retraction of mature rods locally drives age-related synaptic remodeling.

Active AMPK attenuates synaptic aging

The occurrence of age-related changes in young AMPK-deficient mice, together with the marked decrease in AMPK activation in old wild-type animals, suggests that this signaling pathway may provide a target for suppressing synaptic changes in old animals. To test this idea, we asked whether retinal alterations can be reversed in old wild-type and young adult *Lkb1*^{ret} and *Lkb1*^{rod} animals by directly enhancing AMPK activity. We infected photoreceptors with AAV2/5 CA-AMPK after synaptic remodeling had developed and quantified the number of ectopic synapses 3 months later. CA-AMPK decreased synaptic remodeling by 17–25% in *Lkb1*^{ret}, *Lkb1*^{rod} and old mice (Fig. 7a–d). Thus, active AMPK can directly reduce age-related remodeling.

We next asked whether altering the activity of the LKB1-AMPK axis through dietary or therapeutic interventions could affect synaptic aging. We tested three regimens known to modulate this signaling pathway: metformin[38], caloric restriction and a high-fat diet[39]. Quantification of synaptic remodeling showed that metformin treatment reduced ectoptic synapse remodeling by ~20% relative to aged control animals (Fig. 7e,f). In parallel, separate cohorts of animals were subjected to calorically restricted or high-fat diets. Caloric restriction reduced the formation of ectopic synapses in outer retinas of old mice by 50% relative to age-matched controls fed *ad libitum* (Fig. 7g,h) and restored pAMPK levels (Fig. 7i,j). Conversely, a high-fat diet increased synaptic mislocalization by 70% (Fig. 7h). Thus, modulating energy homeostasis either genetically or pharmacologically can help to restore appropriate synaptic localization in old age.

DISCUSSION

Our results suggest that LKB1 and its substrate AMPK are involved in age-related remodeling of retinal synapses. In support of this conclusion, we found that levels of LKB1 and active (phosphorylated) AMPK were reduced in old retina (Fig. 3), deletion of LKB1 or AMPK led to changes resembling those in old retina both qualitatively and quantitatively (Figs. 1 and 4, and Supplementary Figs. 1–3), expression of constitutively active AMPK in old retina attenuated age-related synaptic alterations (Fig. 7a–d), and treatments known to increase AMPK activity (metformin and caloric restriction) also attenuated these alterations (Fig. 7e,h). Combining genetic and imaging methods, we found that LKB1 and AMPK acted primarily in rod photoreceptors to initiate a multicellular cascade leading to axon retraction and synaptic reorganization (Figs. 2, 5 and 6). Together, these results provide insights into both the molecular and cellular bases for synaptic aging and suggest strategies that could be used to attenuate these alterations.

The LKB1-AMPK axis regulates synaptic aging

Deletion of either LKB1 or AMPK resulted in synaptic remodeling that quantitatively and qualitatively mirrored the changes that we documented in old age. These parallels include photoreceptor axon retraction, sprouting of horizontal and bipolar cell processes, cofasiculation of horizontal and bipolar cell sprouts, formation of ultrastructurally and molecularly differentiated ectopic synapses in the outer nuclear layer, involvement of rods and their synaptic partners, but not cones and their synaptic partners, decreased OPL thickness, and functional deficits as measured by ERGs. Moreover, the numbers of interneuronal sprouts and ectopic synapses and the length of these sprouts are similar in old and mutant retinas. Thus, although other genes certainly participate in age-related synaptic remodeling, our data suggest that the LKB1-AMPK axis represents a major outer retina synapse maintenance pathway. These kinases are known to regulate lifespan in worms and flies[15,16], but they have not been considered to be synaptic maintenance regulators in any species.

Our results also address whether the roles of AMPK and LKB1 are specific. Phosphorylation of AMPK by LKB1 is essential for AMPK activity. However, LKB1 phosphorylates and activates 13 additional AMPK-related kinases[11,40], and although AMPK is a major substrate of LKB1, its activity is regulated through a variety of LKB1- independent pathways. Two lines of evidence suggest that AMPK is the major LKB1 target required for synaptic maintenance in old age. First, whereas activation of AMPK, MARK and SAD kinases (MARK1–4, SAD-A and SAD-B) all greatly decreased in LKB1 mutants, only AMPK exhibited decreased activation (T loop phosphorylation) in old retina. Second, no retinal defects were apparent in SAD-A and SAD-B double mutants, even though they display substantial defects in neuronal polarization and axonal arborization in other parts of the nervous system[12,30,41]. Notably, this specificity is unlikely to reflect restricted expression patterns, as we and others have shown that SAD kinases and other LKB1 targets are broadly expressed[12,41].

In contrast, it seems unlikely that the marked age-related decline in AMPK activity is completely a result of the modest decrease in LKB1 levels. One possibility is that the ability of LKB1 to activate AMPK is decreased more than expected from the reduction in LKB1 protein levels. For example, LKB1 might be mislocalized or hindered in its ability to interact with its obligate cofactors, STRAD and MO25 (ref. 11). Alternatively, alterations in the levels of metabolites might affect the ability of AMPK to serve as a substrate for LKB1. Increased ratios of AMP to ATP result in an AMP-mediated structural shift that exposes the T-loop activation site in the AMPKα subunit, the phosphorylation of which is required for AMPK catalytic activity. Yet another possibility is that other kinases that can phosphorylate the AMPK T-loop, such as TAK1 and CAMKK, are affected in old retina. However, conditional TAK1 deletion did not result in age-related synaptic changes, and we found no decrease in CAMKKα/β levels in old retina (data not shown). In addition, the decreased phosphorylation of AMPK in LKB1 mutant retina indicates that in this tissue, as in many others, LKB1 is the major AMPK-activating kinase. Together, these results suggest that decreased activation of AMPK by LKB1 is a major driver of synaptic remodeling in old

retina, but that the decreased activation results not only from loss of LKB1, but also from a decrease in the ability of AMPK to serve as an LKB1 substrate.

Rods retraction drives synaptic remodeling

Synaptic remodeling in old outer retina involves alterations in three neuronal types: photoreceptors, horizontal cells and bipolar cells. Because the photoreceptor synapse is exceptionally large, we were able to analyze all three of the synaptic partners using light microscopy with a level of detail that would not be possible at most brain synapses. This analysis revealed, unexpectedly, that a major cellular feature of age-related remodeling is the retraction of rod photoreceptor terminals. We provide several lines of evidence suggesting that this process leads secondarily to postsynaptic remodeling. First, in old and LKB1 mutant retinas, rod photoreceptor terminals retracted, but cone photoreceptor terminals did not. Second, deletion of LKB1 or AMPK from rods alone phenocopied the entire spectrum of alterations seen in old retina. Third, the level of interneuronal sprouting could be quantitatively accounted for by the incidence of rod retraction. Fourth, when LKB1 or AMPK was deleted from only a few rods, it was apparent that horizontal and bipolar cell processes sprout in direct apposition to the retracted rod terminals. Finally, synaptic partners of rods, rod bipolars and horizontal cell axons, sprouted in old retina, whereas synaptic partners of cones, cone bipolars and horizontal cell dendrites, did not. Thus, consistent with their role in axon formation during development[12,28,29], LKB1 and AMPK are needed to maintain axonal integrity in old age.

Although our data indicate that bipolar and horizontal cells respond to LKB1/AMPK-induced alterations in rods, it remains unclear how alterations in rods lead to interneuron sprouting. One simple possibility is that interneuronal processes remain adhesive to retracting photoreceptor terminals and are thereby pulled into the outer nuclear layer; once there, they might make *en passant* synapses on nearby photoreceptor axons. A second possibility is that retracting rods release a ‘sprouting factor’, as has been postulated for the skeletal neuromuscular junction[42]. A third possibility is that presynaptic alterations may lead to decreases in neurotransmitter release that are sensed by postsynaptic partners and lead to their sprouting. Consistent with this model, mutation of several genes implicated in photoreceptor synaptic transmission, including *Bassoon* and *Cacna1f*, also lead to sprouting of bipolar and horizontal cells[24–27,43,44]. Thus, although loss or delocalization of Bassoon and other structural components of synapses are not detectable in old retina, we speculate that decreased AMPK activity may act in part by decreasing synaptic transmission from rods to their targets. Indeed, synaptic transmission from rods decreases in old age[21] and AMPK affects neuron excitability and firing rates[45]. Moreover, the similarity of changes in Bassoon and CACNA1f mutants to those in old animals suggests that rod retraction may represent a common mechanism on which these pathways converge. In preliminary single neuron–labeling studies, we have observed axon retraction in rods lacking Bassoon (S. Sarin and J.R.S., unpublished data).

Implications for preventing and reversing synaptic aging

Three methods of increasing AMPK activity attenuated synaptic alterations in old retina: expression of CA-AMPK, administration of metformin and caloric restriction. Among these,

caloric restriction was the most effective, leading to a ~50% decrease in ectopic synapse formation. This could imply that other factors in addition to AMPK are involved, but may merely reflect the fact that caloric restriction affects all rods, whereas only a small fraction of the photoreceptors were transduced by active AMPK in our experiments. We also found that CA-AMPK can decrease synaptic remodeling even in cases in which ectopic synapses have already formed, indicating that connectivity between rods and their postsynaptic partners remains flexible once miswiring develops. Thus, activation of AMPK may be able to slow and even reverse age-related synaptic decline.

Identification of the LKB1-AMPK pathway as a regulator of synaptic aging was facilitated by our use of photoreceptor synapses: these connections are particularly large, accessible and well characterized, and specific labels are available that mark all of the synaptic partners. An obvious question is whether this pathway also underlies age-related alterations in the smaller and less accessible synapses in other parts of the CNS. Although more challenging, newer higher resolution microscopy techniques could be brought to bear on this question. Favoring this possibility, caloric restriction, which acts in part through AMPK[46], attenuates age-related cognitive decline in rodents and humans[47] as well as age-related structural alterations at peripheral neuromuscular junction synapses[48]. If further analysis supports this idea, the LKB1-AMPK pathway could be an attractive target for interventions aimed at mitigating age-related synaptic decline.

ONLINE METHODS

Mouse strains

Old (24–30 months) and young adult (3–5 months) C57BL/6J wild-type mice were bred in our vivarium or obtained from the National Institute on Aging or the Jackson Laboratory. The *Lkb1* conditional null mutant (*Lkb1*$^{F/F}$) has been described previously[20] (provided by R. DePinho, Dana-Farber Cancer Research Institute). In this animal, *loxP* sequences flank exons 2–6, resulting in a translational frameshift and complete loss of LKB1 function. To broadly delete *Lkb1* in the retina, *Lkb1*$^{F/F}$ mice were crossed to *Six3-Cre*[49] (provided by W. Kline, Anderson Cancer Center), *Chx10-Cre*[50] (provided by C. Cepko, Harvard University) or *Pax6-Cre*[51] (provided by P. Gruss, Max Planck Institute) mice to generate animals generally referred to here as *Lkb1*^{ret} mice. Similar remodeling phenotypes were observed in all LKB1-deficient crosses. All imaging and quantitative histological analysis was performed with *Lkb1*$^{F/F}$ × *Chx10-cre* animals. RdpsCre[23] mice were crossed to *Lkb1*$^{F/F}$ animals to delete *Lkb1* in rod photoreceptors. Mice carrying the *loxP*-flanked allele of *Tak1* (*Tak1*$^{F/F}$), another AMPK phosphorylating kinase[52], have been described previously[53] (provided by M. Schneider, Imperial College London) and were crossed to *Nestin-Cre* animals[54] (provided by A. McMahon, Harvard University) to broadly delete *Tak1* in the retina. Conditional *SAD-A/B* animals were generated by in our laboratory[41] and were crossed to *Chx10-Cre* animals to generate *Sad-A/B*–deficient retinas for analysis.

The *Ampka1*$^{F/F}$ × *Ampka2*$^{F/F}$ double conditional null mutants (*Ampk*$^{F/F}$) were generated by crossing *Ampka1*$^{F/F}$ and *Ampka2*$^{F/F}$ animals (provided by M. Foretz and B. Viollet, Université Paris Descartes). In the *Ampka1* line, *loxP* sequences flank exons 4 and 5, which include the catalytic domain (M. Foretz, unpublished data), whereas, in the *Ampka2* line,

loxP sequences flank exon C, which encodes the catalytic domain of AMPKα2 (ref. 55). Experiments were carried out in accordance with protocols approved by the Harvard University Standing Committee on the Use of Animals in Research and Teaching.

Tissue preparation and immunohistochemistry

Mice were anesthetized with Nembutal and either enucleated directly or perfused with phosphate-buffered saline (PBS) followed by 4% paraformaldehyde (wt/vol) in PBS. Eyes were collected and fixed for 30 min in paraformaldehyde on ice and then rinsed with PBS. Cryosections and whole-mount retinas were prepared as described[5]. Briefly, sections were incubated in blocking solution (3% normal donkey serum and 0.3% Triton X-100 (vol/vol) in PBS), followed by incubation with primary and secondary antibodies (Invitrogen or Jackson ImmunoResearch). Following washing, sections were mounted in Vectashield (Vectorlabs). Retinas from 3–9 mice were analyzed in each experimental group.

The primary antibodies in this study recognized the following molecules: calbindin (1:2,500, CB38a, Swant), GFP (1:1,000, AB16901, Chemicon), protein kinase Cα (PKCα, 1:500, ab31, AbCam), potassium/sodium hyperpolarization-activated cyclic nucleotide-gated channel 4 (HCN4, 1:500, 75–150, Neuromabs), calsenilin (KChip, 1:100, 75-005, Neuromabs), cre (1:500, MMS-106P, Covance), mouse cone arrestin (mCAR, 1:1,000, provided by C. Craft, University of Southern California[56]), recoverin (1:4,000, AB5585, Millipore), protein kinase A, regulatory subunit IIβ (PKARIIb, 1:1,500, 610625, BD Biosciences), PSD-95 (1:200, MA1-046, Thermo Scientific), RIBEYE (1:500, 192 003, Synaptic Systems), Bassoon (1:500, VAM-PS003, Enzo Life Sciences), Piccolo (1:500, 142 003, Synaptic Systems), dystrophin (1:20, NCL-DYS2, Novacastra), and dihydropyridine-sensitive calcium channel α1 subunit (CACNA1, 1:2,000, MAB427, Millipore. TO-PRO-3 (Invitrogen) was used to visualize nuclei. Images were acquired on an Olympus FluoView FV1000 confocal microscope and processed using ImageJ.

ERG recording

ERGs were recorded from adult (8–9 months old) control *Lkb1*$^{F/F}$ mice ($n = 6$), *Lkb1*$^{F/F}$ × *Chx10-Cre* mice ($n = 4$), and *Lkb1*$^{F/F}$ × *Six3-Cre* mice ($n = 4$). Mice were dark-adapted overnight and anesthetized with sodium pentobarbital injected intraperitoneally before testing. Both pupils of each animal were topically dilated with phenylephrine hydrochloride and cyclopentolate hydrochloride, and mice were then placed on a heated platform. Rod dominated responses were elicited in the dark with 10-μs flashes of white light (1.37×10^5 cd m^{-2}) presented at intervals of 1 min in a Ganzfeld dome. Light-adapted cone responses were elicited with the same flashes presented at 1 Hz in the presence of a 41 cd m^{-2} rod-desensitizing white background. ERGs were monitored from both eyes simultaneously with a silver wire loop electrode in contact with each cornea topically anesthetized with proparacaine hydrochloride and wetted with Goniosol and with a saline-soaked cotton wick in the mouth as the reference; an electrically shielded chamber served as ground.

All responses were differentially amplified at a gain of 1,000 (-3 db at 2 Hz and 300 Hz; AM502, Tektronix Instruments), digitized at 16-bit resolution with an adjustable peak-to-peak input amplitude (PCI-6251, National Instruments), and displayed on a personal

computer using custom software (Labview, version 8.2, National Instruments). Independently for each eye, cone responses were conditioned by a 60-Hz notch filter and an adjustable artifact-reject window and were summed (n = 4–20).

Electron microscopy

Eyecups were fixed successively in 4% paraformaldehyde, 2% glutarladehyde for 2 h, in 2% paraformaldehyde, 4% glutarladehyde for 1 h, and in 4% glutarladehyde overnight (wt/vol). All solutions were prepared in 0.1 M cacodylate buffer. Samples were rinsed in 0.1 M cacodylate buffer and then osmicated in 2% OsO_4 (wt/vol) overnight. Ultrathin sections were cut on a Leica EMS ultramicrotome to a thickness of 50 nm using a Diatome 45 degree Ultracut diamond knife and were collected on 1 × 2 mm slotted grids coated with formvar and carbon. The sections were allowed to dry and were then stained with 2% uranyl acetate (wt/vol) for 15 min. They were washed three times, stained with stabilized Reynold's lead citrate solution for 10 min and washed again three times. Sections were imaged using an FEI Tecnai G2 Spirit transmission electron microscope equipped with a Gatan camera.

AAV-mediated neuron labeling and single cell deletion

For AAV-mediated neuron labeling, young adult control, Lkb^{ret}, $Lkb1^{rod}$ (3–5 months) and old (24–28 months) mice were anaesthetized by intraperitoneal injection of ketamine/xylene (1.7 mg per 20 g of body weight). To label individual horizontal cells, the sub-retinal space was inoculated with AAV2/2-YC3.6 (viral stocks generated by the Harvard Gene Therapy Institute). YC3.6 is a calcium sensor that combines YFP and CFP[57], but in this study was used only for labeling[58]. To label individual photoreceptors, the subretinal space was inoculated with AAV2/5-GFP (prepared at the Harvard Gene Therapy Institute). Mice were infected as previously described[59] using virus diluted to an experimentally determined optimal titer for single cell labeling (10^9 to 10^{10} viral genome particles per ml).

To delete LKB1 from individual photoreceptors, young adult $Lkb1^{F/F}$, $Ampka1^{F/F}$ × $Ampka2^{F/F}$ or control animals (2 months) were infected with AAV2/5-Cre (Vector BioLabs) to induce either sparse (~10^{10} viral genome particles per ml) or dense (undiluted) deletion. All animals were killed 5–8 weeks after infection. No remodeling was observed in control experiments.

Histological quantification

All quantification was performed using retinal sections prepared from young control, $Lkb1^{ret}$, $Lkb1^{rod}$, or $Ampka1^{F/F}$ × $Ampka2^{F/F}$ animals (3–5 months) and old mice (24–28 months). To quantify the thickness of the OPL, images were acquired at equivalent retinal eccentricities from the optic nerve head. Layer width was measured using ImageJ in 5–10 non-consecutive single optical planes per image, from at least four image stacks per retina and from four animals per group. To determine the number of total and ectopically localized Bassoon-positive puncta, retinal sections were stained using antibody to Bassoon and the nuclear marker TO-PRO-3 and imaged at high resolution at equivalent retinal eccentricities. An ectopic synapse was defined as a Bassoon-positive puncta localized at least one nucleus above the OPL. The number of total and ectoptic puncta were determined in single optical sections using ImageJ. Data were collected from 4–8 mice per group. Four images per retina

were analyzed, and puncta were quantified from 5–10 non-successive optical sections per image stack. To quantify the number and length of neurite sprouts, retinal sections were stained for rod bipolar cells using PKCα together with TO-PRO-3. The number and length of neurite sprouts were determined in 5–8 single optical planes at least 3 μm apart. 3–4 images per retina were analyzed from five mice per group. To quantify the percentage of retracted rods, rod terminals were visualized using AAV2/5 to label single neurons together with staining for the nuclear marker TO-PRO-3 and the rod terminal marker PSD95. The total number of labeled terminals and the number of those retracted within the ONL were quantified in 5–8 single optical planes at least 2 μm apart. Three to four images per retina were analyzed from three mice per group. All data were analyzed using Prism Graphpad. Quantification results are represented as bar graphs where error bars represent the s.e.m.

In situ hybridization

In situ hybridization was performed as previously decribed[60]. To generate the *Lkb1* probes, LKB1 (provided by F. Polleux[12], Columbia University) was subcloned into pGEM-T Easy (Promega). Antisense probe and sense controls were generated by linearizing with NcoI and Sae1, respectively. *Ampkα2* antisense probe was generated using an AMPKα2 clone from Addgene (Plasmid 15991), which was linearized using MfeI. Antisense riboprobes were transcribed using the DIG RNA labeling kit (Roche).

Immunoblotting and analysis

To analyze protein levels in total retina, individual retina were dissected in cold Tris-buffered saline and then immediately lysed in 100 μl of denaturing buffer (100 mM Tris-HCl, 10 mM magnesium acetate, 6 M urea, 2% SDS (wt/vol)) containing complete EDTA-free protease inhibitors (Roche), phosphatase inhibitor cocktails I and II (Calbiochem), and Benzoase nuclease (25 U ml^{-1}, Novagen). Retina were homogenized using a handheld mixer pestle and motor (VWR). To assay protein levels in photoreceptors, retinas were dissociated using papain[61], fixed (Paxgene, Qiagen), and then stained for the photoreceptor marker recoverin. Recoverin-positive cells were isolated using an Astrios cell sorter. Cells were pelleted and then lysed in denaturing buffer as described above. All homogenates were heated at 95 °C for 5 min and then centrifuged (10,000*g* for 5 min). Protein concentrations were determined by BCA assay (Pierce), and aliquots were stored at -80 °C. Equal amounts of protein (15–20 μg) were analyzed by SDS-PAGE analysis on gradient resolving gels (Thermo). Protein was then transferred to a polyvinylidene difluoride (PVDF) membrane (Millipore), blocked for 1 h at ~25°C in 5% BSA (wt/vol) in Tris-buffered saline, and then incubated overnight at 4 °C with primary antibody. The primary antibodies used for immunoblot analyses were as follows: LKB1 (1:700, 07-694, Upstate), pMARK1-4 (1:1,000, 4836, Cell Signaling), pSAD-A/B (1:5,000)[12], pAMPK, Thr172 (1:1,000, 2531, Cell Signaling), AMPK (1:1,000, 2532, Cell Signaling), pACC, Ser79 (1:1,000, 3661, Cell Signaling), Bassoon (1:1,000, VAM-PS003, Enzo Life Sciences), CACNA1f (1:1,000, LS-C94032, Lifespan Biosciences), and GAPDH (1:5,000, MAB374, Millipore). Membranes were then washed, incubated with appropriate HRP-tagged secondary antibodies (1:30,000, 115-035-146 and 115-035-144, Jackson ImmunoResearch), and then developed. Protein bands were quantified and normalized using ImageJ. Two or more independent experiments

from 4–18 animals per group were performed for all immunoblot data. Quantification results are represented as bar graphs where error bars represent the s.e.m.

Therapeutic regimens

A plasmid encoding AMPKα2 was obtained from Addgene (Plasmid 15991), and site-directed mutagenesis was performed to mutate the activating threonine at 172 to glutamic acid, which mimics phosphorylation and renders AMPK constitutively active (CA-AMPK[33]). Appropriate mutagenesis was validated by sequencing. Plasmid encoding CA-AMPK was used to generate recombinant AAV2/5 expressing CA-AMPK under the control of a CMV promoter (AAV2/5CA-AMPK, prepared by the Harvard Gene Therapy Institute).

For synaptic remodeling prevention studies, newborn (P1) *Lkb1*^{rod} animals were anesthetized using ice, and a small incision was made in the eyelid with a 30-gauge needle. A mixture of AAV2/5CA-AMPK and AAV2/5GFP (as a tracer) was injected into the subretinal space through the incision using a pulled glass pipette. For synaptic remodeling reversal studies, the AAV2/5CA-AMPK solution was injected into the subretinal space of old mice (24–26 months), as well as adult (2–3 months) controls and *Lkb1*^{rod} and *Lkb1*^{ret} animals as described above. In both prevention and reversal studies, the level of synaptic remodeling in infected and uninfected internal control regions of the same retinas were determined 2 months after infection.

To analyze the effects of metformin and diet on age-related synaptic alterations, we obtained five sets of C57BL/6 mice from the National Institute of Aging: 24-month-old mice that had been fed a standard diet *ad libitum*, and 24-month-old mice that had been fed a calorically restricted diet[62], mice that had been maintained on a high fat diet (60% of calories from fat), untreated animals (metformin controls) and animals that had been treated with metformin (0.1%, wt/vol). Synaptic remodeling was assessed in retinas from these animals as described above.

Statistical analysis

Histological and immunoblot data were compared using an unpaired, two-tailed Student's *t* test unless otherwise noted and evaluated using Prism software (GraphPad). Data distribution was assumed to be normal but this was not formally tested. ERG amplitudes were transformed to natural logarithms, and group means (that is, for *Lkb1*^{ret} mice versus control mice) were compared with PROC MIXED of SAS, version 9.3 (SAS Institute) by repeated measures regression using the eye as the unit of analysis and allowing for unequal variances. No statistical methods were used to pre-determine sample sizes, but our samples sizes are consistent with those generally employed in the field. Randomization and blinding were not employed in data collection and analysis.

A **Supplementary methods checklist** is available.

Supplementary Material

Refer to Web version on PubMed Central for supplementary material.

Acknowledgments

We thank members of our laboratory for scientific discussions and advice, and A. Thanos for help with the AMPK animals. This work was funded by the US National Institutes of Health (AG32322 to J.R.S. and 5K99AG044444 to M.A. Samuel), the Damon Runyon Cancer Research Foundation (M.A. Samuel), Research to Prevent Blindness (J.R.S. and D.G.V.), the Foundation Fighting Blindness (B.P.), and the Intramural Research Program of the National Institute on Aging (R.d.C.).

References

1. Burke SN, Barnes CA. Neural plasticity in the ageing brain. Nat Rev Neurosci. 2006; 7:30–40. [PubMed: 16371948]
2. Morrison JH, Baxter MG. The ageing cortical synapse: hallmarks and implications for cognitive decline. Nat Rev Neurosci. 2012; 13:240–250. [PubMed: 22395804]
3. Scheff SW, Price DA. Synaptic pathology in Alzheimer's disease: a review of ultrastructural studies. Neurobiol Aging. 2003; 24:1029–1046. [PubMed: 14643375]
4. Scheff SW, Price DA, Schmitt FA, DeKosky ST, Mufson EJ. Synaptic alterations in CA1 in mild Alzheimer disease and mild cognitive impairment. Neurology. 2007; 68:1501–1508. [PubMed: 17470753]
5. Samuel MA, Zhang Y, Meister M, Sanes JR. Age-related alterations in neurons of the mouse retina. J Neurosci. 2011; 31:16033–16044. [PubMed: 22049445]
6. Liets LC, Eliasieh K, van der List DA, Chalupa LM. Dendrites of rod bipolar cells sprout in normal aging retina. Proc Natl Acad Sci USA. 2006; 103:12156–12160. [PubMed: 16880381]
7. Eliasieh K, Liets LC, Chalupa LM. Cellular reorganization in the human retina during normal aging. Invest Ophthalmol Vis Sci. 2007; 48:2824–2830. [PubMed: 17525218]
8. Terzibasi E, et al. Age-dependant remodeling of retinal circuitry. Neurobiol Aging. 2009; 30:819–828. [PubMed: 17920161]
9. Sanes JR, Zipursky SL. Design principles of insect and vertebrate visual systems. Neuron. 2010; 66:15–36. [PubMed: 20399726]
10. Masland RH. The fundamental plan of the retina. Nat Neurosci. 2001; 4:877–886. [PubMed: 11528418]
11. Alessi DR, Sakamoto K, Bayascas JR. LKB1-dependent signaling pathways. Annu Rev Biochem. 2006; 75:137–163. [PubMed: 16756488]
12. Barnes AP, et al. LKB1 and SAD kinases define a pathway required for the polarization of cortical neurons. Cell. 2007; 129:549–563. [PubMed: 17482548]
13. Shelly M, Cancedda L, Heilshorn S, Sumbre G, Poo MM. LKB1/STRAD promotes axon initiation during neuronal polarization. Cell. 2007; 129:565–577. [PubMed: 17482549]
14. Mirouse V, Billaud M. The LKB1/AMPK polarity pathway. FEBS Lett. 2011; 585:981–985. [PubMed: 21185289]
15. Funakoshi M, et al. A gain-of-function screen identifies wbd and lkb1 as lifespan-extending genes in *Drosophila*. Biochem Biophys Res Commun. 2011; 405:667–672. [PubMed: 21281604]
16. Narbonne P, Roy R. *Caenorhabditis elegans* dauers need LKB1/AMPK to ration lipid reserves and ensure long-term survival. Nature. 2009; 457:210–214. [PubMed: 19052547]
17. Houtkooper RH, Williams RW, Auwerx J. Metabolic networks of longevity. Cell. 2010; 142:9–14. [PubMed: 20603007]
18. Cai Z, Yan LJ, Li K, Quazi SH, Zhao B. Roles of AMP-activated protein kinase in Alzheimer's disease. Neuromolecular Med. 2012; 14:1–14. [PubMed: 22367557]
19. Ollila S, Mäkelä TP. The tumor suppressor kinase LKB1: lessons from mouse models. J Mol Cell Biol. 2011; 3:330–340. [PubMed: 21926085]
20. Bardeesy N, et al. Loss of the Lkb1 tumour suppressor provokes intestinal polyposis but resistance to transformation. Nature. 2002; 419:162–167. [PubMed: 12226664]
21. Kolesnikov AV, Fan J, Crouch RK, Kefalov VJ. Age-related deterioriation of rod vision in mice. J Neurosci. 2010; 30:11222–11231. [PubMed: 20720130]

22. Palczewski K. Chemistry and biology of vision. J Biol Chem. 2012; 287:1612–1619. [PubMed: 22074921]
23. Li S, et al. Rhodopsin-iCre transgenic mouse line for Cre-mediated rod-specific gene targeting. Genesis. 2005; 41:73–80. [PubMed: 15682388]
24. Dick O, et al. The presynaptic active zone protein bassoon is essential for photoreceptor ribbon synapse formation in the retina. Neuron. 2003; 37:775–786. [PubMed: 12628168]
25. Mansergh F, et al. Mutation of the calcium channel gene Cacna1f disrupts calcium signaling, synaptic transmission and cellular organization in mouse retina. Hum Mol Genet. 2005; 14:3035–3046. [PubMed: 16155113]
26. Chang B, et al. The nob2 mouse, a null mutation in Cacna1f: anatomical and functional abnormalities in the outer retina and their consequences on ganglion cell visual responses. Vis Neurosci. 2006; 23:11–24. [PubMed: 16597347]
27. Specht D, et al. Structural and functional remodeling in the retina of a mouse with a photoreceptor synaptopathy: plasticity in the rod and degeneration in the cone system. Eur J Neurosci. 2007; 26:2506–2515. [PubMed: 17970721]
28. Amato S, et al. AMP-activated protein kinase regulates neuronal polarization by interfering with PI3-kinase localization. Science. 2011; 332:247–251. [PubMed: 21436401]
29. Williams T, Courchet J, Viollet B, Brenman JE, Polleux F. AMP-activated protein kinase (AMPK) activity is not required for neuronal development but regulates axogenesis during metabolic stress. Proc Natl Acad Sci USA. 2011; 108:5849–5854. [PubMed: 21436046]
30. Kishi M, Pan YA, Crump JG, Sanes JR. Mammalian SAD kinases are required for neuronal polarization. Science. 2005; 307:929–932. [PubMed: 15705853]
31. Biernat J, et al. Protein kinase MARK/PAR-1 is required for neurite outgrowth and establishment of neuronal polarity. Mol Biol Cell. 2002; 13:4013–4028. [PubMed: 12429843]
32. Hardie DG, Ross FA, Hawley SA. AMPK: a nutrient and energy sensor that maintains energy homeostasis. Nat Rev Mol Cell Biol. 2012; 13:251–262. [PubMed: 22436748]
33. Woods A, et al. Identification of phosphorylation sites in AMP-activated protein kinase (AMPK) for upstream AMPK kinases and study of their roles by site-directed mutagenesis. J Biol Chem. 2003; 278:28434–28442. [PubMed: 12764152]
34. Kolb H. The connections between horizontal cells and photoreceptors in the retina of the cat: electron microscopy of Golgi preparations. J Comp Neurol. 1974; 155:1–14. [PubMed: 4836060]
35. Wässle H, Puller C, Müller F, Haverkamp S. Cone contacts, mosaics, and territories of bipolar cells in the mouse retina. J Neurosci. 2009; 29:106–117. [PubMed: 19129389]
36. Koulen P, Fletcher EL, Craven SE, Bredt DS, Wässle H. Immunocytochemical localization of the postsynaptic density protein PSD-95 in the mammalian retina. J Neurosci. 1998; 18:10136–10149. [PubMed: 9822767]
37. Brandstätter JH, Fletcher EL, Garner CC, Gundelfinger ED, Wässle H. Differential expression of the presynaptic cytomatrix protein bassoon among ribbon synapses in the mammalian retina. Eur J Neurosci. 1999; 11:3683–3693. [PubMed: 10564375]
38. Shaw RJ, et al. The kinase LKB1 mediates glucose homeostasis in liver and therapeutic effects of metformin. Science. 2005; 310:1642–1646. [PubMed: 16308421]
39. Dagon Y, et al. Nutritional status, cognition and survival: a new role for leptin and AMP kinase. J Biol Chem. 2005; 280:42142–42148. [PubMed: 16203737]
40. Lizcano JM, et al. LKB1 is a master kinase that activates 13 kinases of the AMPK subfamily, including MARK/PAR-1. EMBO J. 2004; 23:833–843. [PubMed: 14976552]
41. Lilley BN, Pan YA, Sanes JR. SAD kinases sculpt axonal arbors of sensory neurons through long- and short-term responses to neurotrophin signals. Neuron. 2013; 79:39–53. [PubMed: 23790753]
42. Brown MC, Holland RL, Hopkins WG. Motor nerve sprouting. Annu Rev Neurosci. 1981; 4:17–42. [PubMed: 7013635]
43. tom Dieck S, et al. Deletion of the presynaptic scaffold CAST reduces active zone size in rod photoreceptors and impairs visual processing. J Neurosci. 2012; 32:12192–12203. [PubMed: 22933801]

44. Haeseleer F, et al. Essential role of Ca^{2+}-binding protein 4, a Cav1.4 channel regulator, in photoreceptor synaptic function. Nat Neurosci. 2004; 7:1079–1087. [PubMed: 15452577]
45. Ikematsu N, et al. Phosphorylation of the voltage-gated potassium channel Kv2.1 by AMP-activated protein kinase regulates membrane excitability. Proc Natl Acad Sci USA. 2011; 108:18132–18137. [PubMed: 22006306]
46. Stenesen D, et al. Adenosine nucleotide biosynthesis and AMPK regulate adult life span and mediate the longevity benefit of caloric restriction in flies. Cell Metab. 2013; 17:101–112. [PubMed: 23312286]
47. Joseph J, Cole G, Head E, Ingram D. Nutrition, brain aging and neurodegeneration. J Neurosci. 2009; 29:12795–12801. [PubMed: 19828791]
48. Valdez G, et al. Attenuation of age-related changes in mouse neuromuscular synapses by caloric restriction and exercise. Proc Natl Acad Sci USA. 2010; 107:14863–14868. [PubMed: 20679195]
49. Furuta Y, Lagutin O, Hogan BL, Oliver GC. Retina- and ventral forebrain-specific Cre recombinase activity in transgenic mice. Genesis. 2000; 26:130–132. [PubMed: 10686607]
50. Rowan S, Cepko CL. Genetic analysis of the homeodomain transcription factor Chx10 in the retina using a novel multifunctional BAC transgenic mouse reporter. Dev Biol. 2004; 271:388–402. [PubMed: 15223342]
51. Marquardt T, et al. Pax6 is required for the multipotent state of retinal progenitor cells. Cell. 2001; 105:43–55. [PubMed: 11301001]
52. Momcilovic M, Hong SP, Carlson M. Mammalian TAK1 activates Snf1 protein kinase in yeast and phosphorylates AMP-activated protein kinase in vitro. J Biol Chem. 2006; 281:25336–25343. [PubMed: 16835226]
53. Liu HH, Xie M, Schneider MD, Chen ZJ. Essential role of TAK1 in thymocyte development and activation. Proc Natl Acad Sci USA. 2006; 103:11677–11682. [PubMed: 16857737]
54. Tronche F, et al. Disruption of the glucocorticoid receptor gene in the nervous system results in reduced anxiety. Nat Genet. 1999; 23:99–103. [PubMed: 10471508]
55. Viollet B, et al. The AMP-activated protein kinase alpha2 catalytic subunit controls whole-body insulin sensitivity. J Clin Invest. 2003; 111:91. [PubMed: 12511592]
56. Zhu X, et al. Mouse cone arrestin expression pattern: light induced translocation in cone photoreceptors. Mol Vis. 2002; 8:462–471. [PubMed: 12486395]
57. Nagai T, Yamada S, Tominaga T, Ichikawa M, Miyawaki A. Expanded dynamic range of fluorescent indicators for Ca(2+) by circularly permuted yellow fluorescent proteins. Proc Natl Acad Sci USA. 2004; 101:10554–10559. [PubMed: 15247428]
58. Hong YK, Kim IJ, Sanes JR. Stereotyped axonal arbors of retinal ganglion cell subsets in the mouse superior colliculus. J Comp Neurol. 2011; 519:1691–1711. [PubMed: 21452242]
59. Lefebvre JL, Kostadinov D, Chen WV, Maniatis T, Sanes JR. Protocadherins mediate dendritic self-avoidance in the mammalian nervous system. Nature. 2012; 488:517–521. [PubMed: 22842903]
60. Kay JN, Voinescu PE, Chu MW, Sanes JR. Neurod6 expression defines new retinal amacrine cell subtypes and regulates their fate. Nat Neurosci. 2011; 14:965–972. [PubMed: 21743471]
61. Lefebvre JL, Zhang Y, Meister M, Wang X, Sanes JR. γ-Protocadherins regulate neuronal survival but are dispensable for circuit formation in retina. Development. 2008; 135:4141–4151. [PubMed: 19029044]
62. Turturro A, et al. Growth curves and survival characteristics of the animals used in the Biomarkers of Aging Program. J Gerontol A Biol Sci Med Sci. 1999; 54:B492–B501. [PubMed: 10619312]

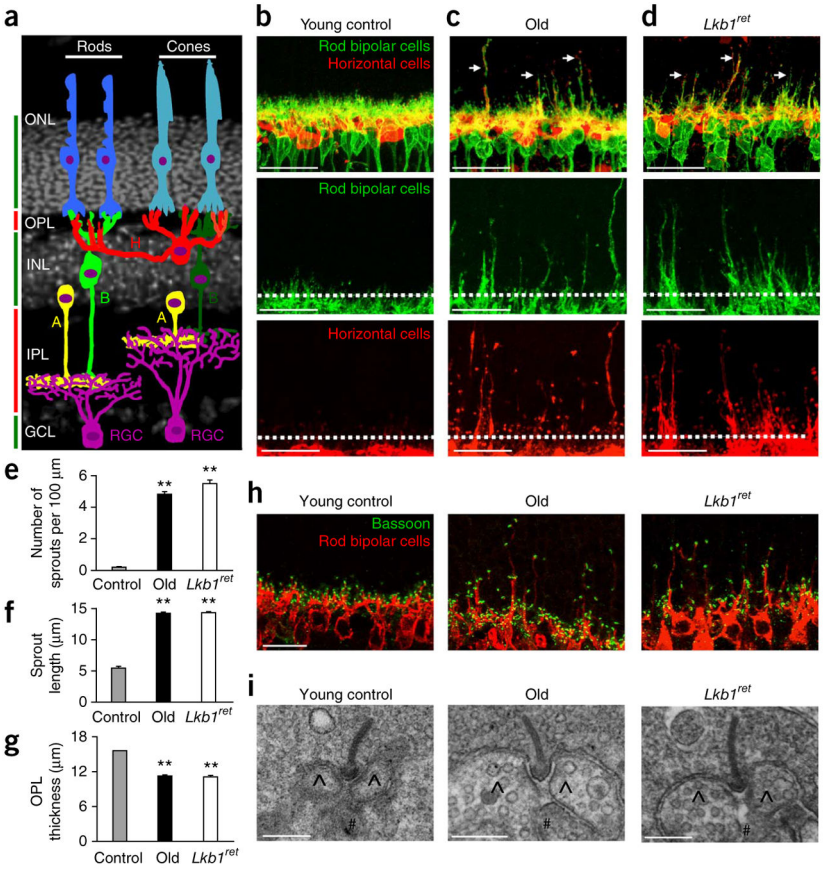

Figure 1.

LKB1 deletion induces age-related changes in young mice. (**a**) Schematic of retinal structure. A, amacrine cell; B, bipolar cell; GCL, ganglion cell layer; H, horizontal cell; INL, inner nuclear layer; IPL, inner plexiform layer; ONL, outer nuclear layer; OPL, outer plexiform layer; RGC, retinal ganglion cell. (**b**–**d**) Lower power (top row, scale bars represent 25 µm) and higher power (middle and bottom rows, scale bars represent 15 µm) images of rod bipolar and horizontal cell ectopic processes (arrows) in young and old wild-type and young *Lkb1*-deficient adult retinas. The dotted line indicates the OPL/ONL border. (**e**,**f**) Number and length of ectopic rod bipolar cell dendrites. Data are presented as mean ± s.e.m. of 45, 81 and 51 (**e**) and 53, 830 and 580 (**f**) measurements from five young control, old and $Lkb1^{ret}$ mice, respectively. (**g**) The OPL thinned to a similar extent in both $Lkb1^{ret}$ and old mice relative to young controls. Data are presented as mean ± s.e.m. of 556, 428 and 262 measurements from four young control, old and $Lkb1^{ret}$ mice, respectively. (**h**) Mislocalized synapses (Bassoon, green) formed along ectopic bipolar processes (PKCα, red). Scale bar represents 15 µm. (**i**) Synapses in the ONL of $Lkb1^{ret}$ and old mice resembled rod spherule synapses in the OPL of young controls by electron microscopy. ^ indicates a bipolar terminal, # indicates a horizontal terminal. Scale bars represent 250 nm. Data were evaluated using an unpaired, two-tailed Student's *t* test. $^{**}P < 0.0001$.

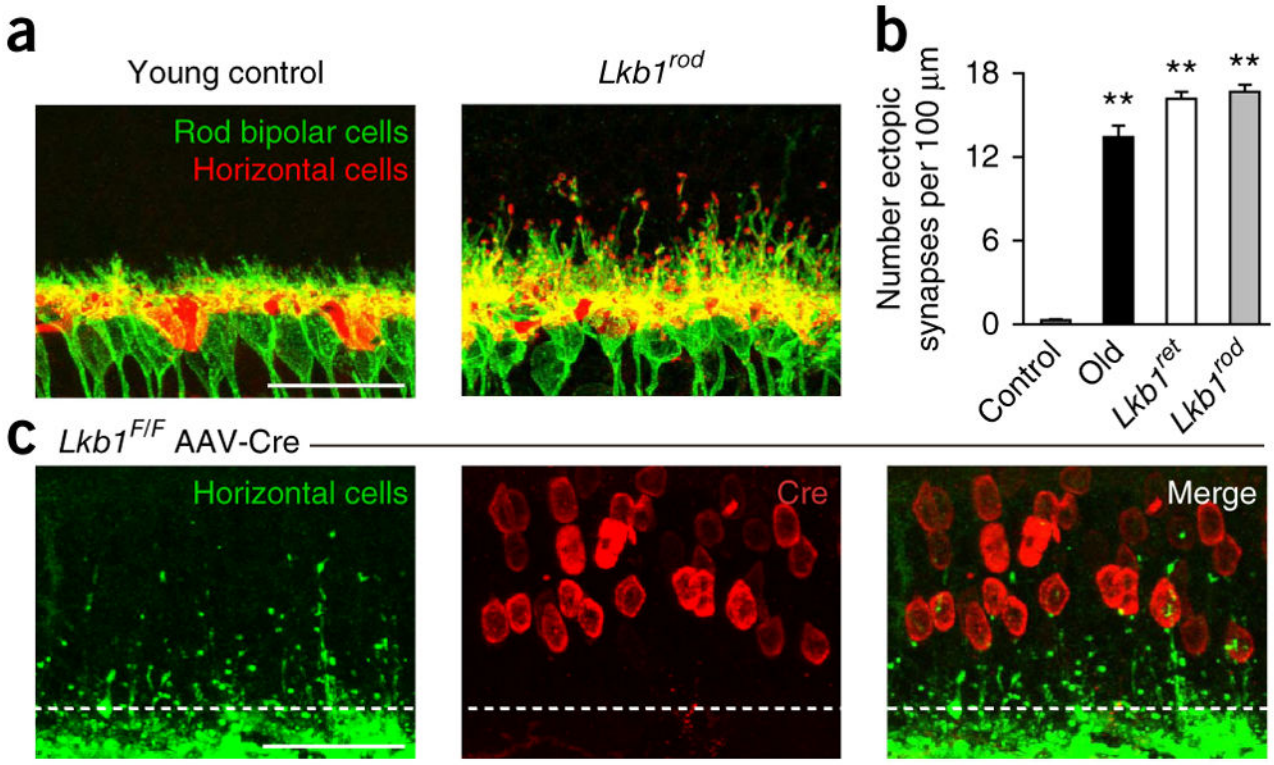

Figure 2.

Rods require LKB1 to maintain synapses in the outer retina. (**a**) *Lkb1* deletion in rods alone (*Lkb1*^{rod}) induced age-related remodeling of rod bipolar and horizontal cells. Scale bar represents 25 µm. (**b**) The number of ectopic synapses in *Lkb1*^{rod} animals is similar to that in *Lkb1*^{ret} and old mice. Data are presented as mean ± s.e.m. of 218, 71, 205 and 183 measurements in young, *Lkb1*^{ret}, *Lkb1*^{rod} and old mice, respectively, from eight young control and knockout animals and four old animals per group. (**c**) *Lkb1* deletion in young adult retina using AAV-Cre induces neurite remodeling. The dashed line indicates the OPL/ONL border. Scale bar represents 25 µm. Data were evaluated using an unpaired, two-tailed Student's *t* test. $^{**}P < 0.0001$.

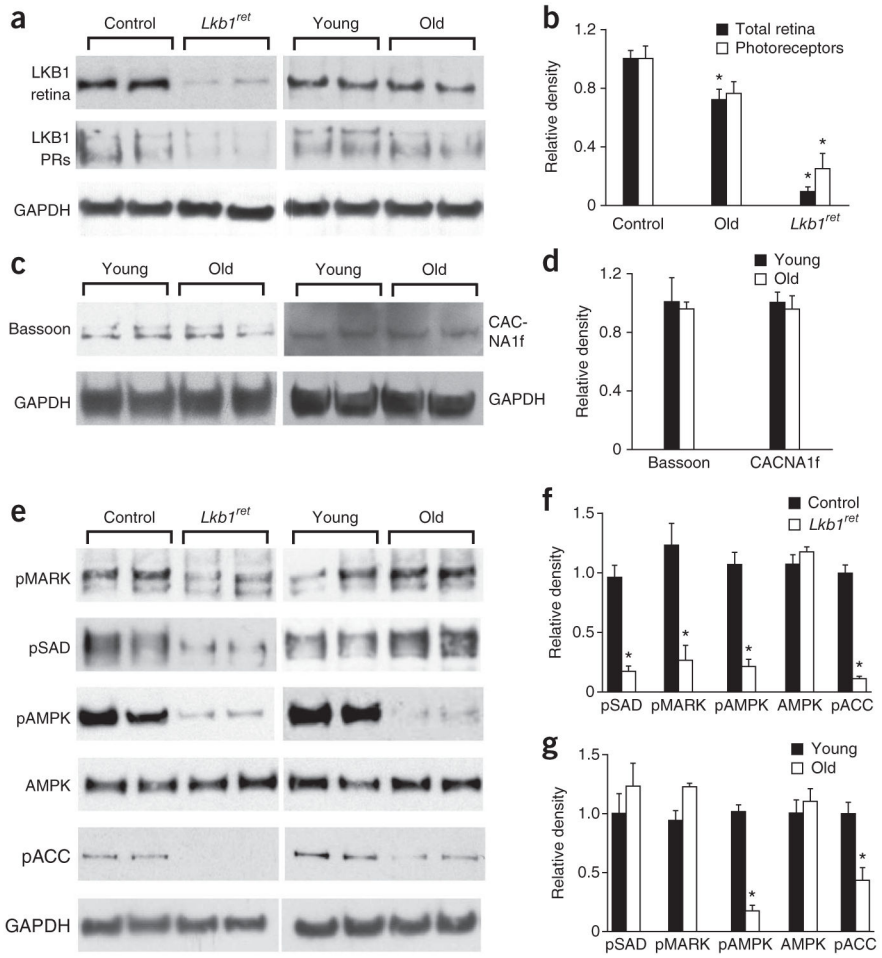

Figure 3.

LKB1-AMPK signaling is disrupted in old age. (**a**,**b**) Levels of LKB1 were reduced in whole retina and in photoreceptors from both *Lkb1*^{ret} and old mice as assayed by immunoblot analysis. Data are presented as mean ± s.e.m. from 18, 17 and 4 control, old (P = 0.004) and *Lkb1*^{ret} (P < 0.0001) animals per group, respectively, for whole retina, and 10, 10 and 4 control, old (P = 0.065) and *Lkb1*^{ret} (P = 0.001) animals per group, respectively, for photoreceptors. (**c**,**d**) The levels of Bassoon and CACNA1f were not significantly altered in old age. Protein levels in whole retina were assayed by immunoblot analysis (**c**, quantified in **d**). Data are presented as mean ± s.e.m. from 4 (Bassoon, P = 0.783) and 7 (CACNA1f, P = 0.703) animals per group. (**e**–**g**) Levels of active phosphorylated SAD-A/SAD-B (pSAD), MARK1–4 (pMARK), AMPK (pAMPK) and ACC (pACC) were reduced in *Lkb1*^{ret} retina, as determined by immunoblot analysis (**e**, quantified in **f**), whereas only pAMPK and its target pACC decreased in old retina (**g**). Data are presented as mean ± s.e.m. from the following sets of control, *Lkb1*^{ret}, young and old animals, respectively: pSAD (n = 6, 6, 4, 4; P < 0.0001), pMARK (n = 6, 4, 4, 4; P = 0.005), pAMPK (n = 12, 4, 9, 8; P = 0.0006 for *Lkb1*^{ret} and P < 0.0001 old animals), AMPK (n = 6, 4, 4, 6); pACC (n = 4, 4, 4, 4; P < 0.0001 for *Lkb1*^{ret} and P = 0.008 for old animals). Full-length blots are presented in

Supplementary Figure 11. Data were evaluated using an unpaired, two-tailed Student's *t* test. $*P < 0.01$.

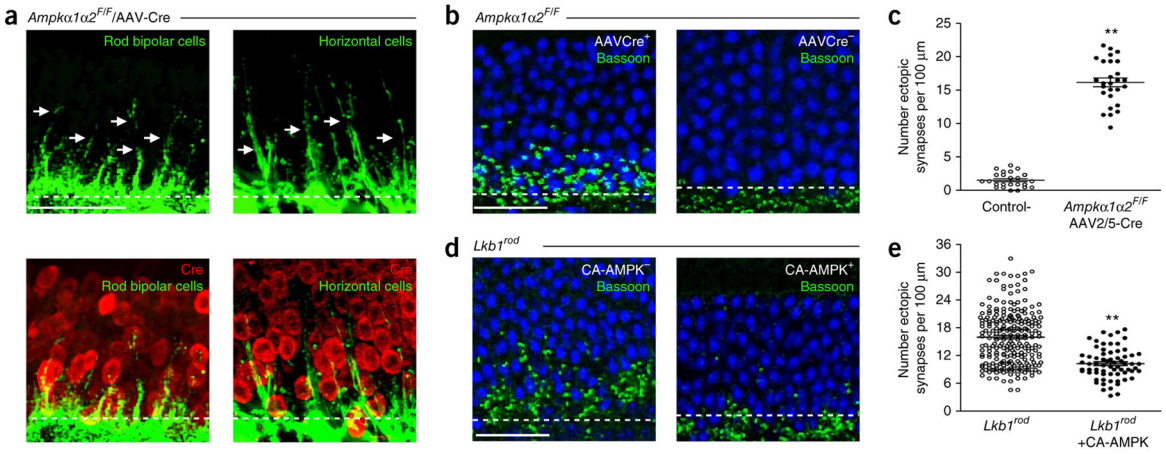

Figure 4.

AMPK acts downstream of LKB1 to maintain retinal synapses. (**a**) Deletion of *Ampkα1* and *Ampkα2* from photoreceptors (*Ampkα1α2*/AAV2/5-Cre) induced remodeling (arrows) of rod bipolar and horizontal cells. Scale bar represents 25 µm. (**b**,**c**) Similar levels of ectopic synapse formation (Bassoon, green) were observed in *Ampkα1α2*/AAV2/5 mice as in old and $Lkb1^{ret}$ animals (**b**, quantified in **c**). Data are presented as mean ± s.e.m. of 26 and 28 fields from 4 animals per group. Scale bar represents 25 µm. (**d**,**e**) CA-AMPK attenuated neural remodeling. $Lkb1^{rod}$ animals were infected with AAV2/5 encoding CA-AMPK at P1, and ectopic synapses (Bassoon, green) were quantified (**d**, scale bar represents 25 µm). CA-AMPK significantly decreased remodeling in infected regions (**e**, data are presented as mean ± s.e.m. of 241 and 68 fields from 8 and 4 $Lkb1^{rod}$ and $Lkb1^{rod}$ + CA-AMPK animals, respectively). Dashed lines indicate the OPL/ONL border. Nuclei, blue. Data were evaluated using an unpaired, two-tailed Student's *t* test. $^{**}P < 0.0001$.

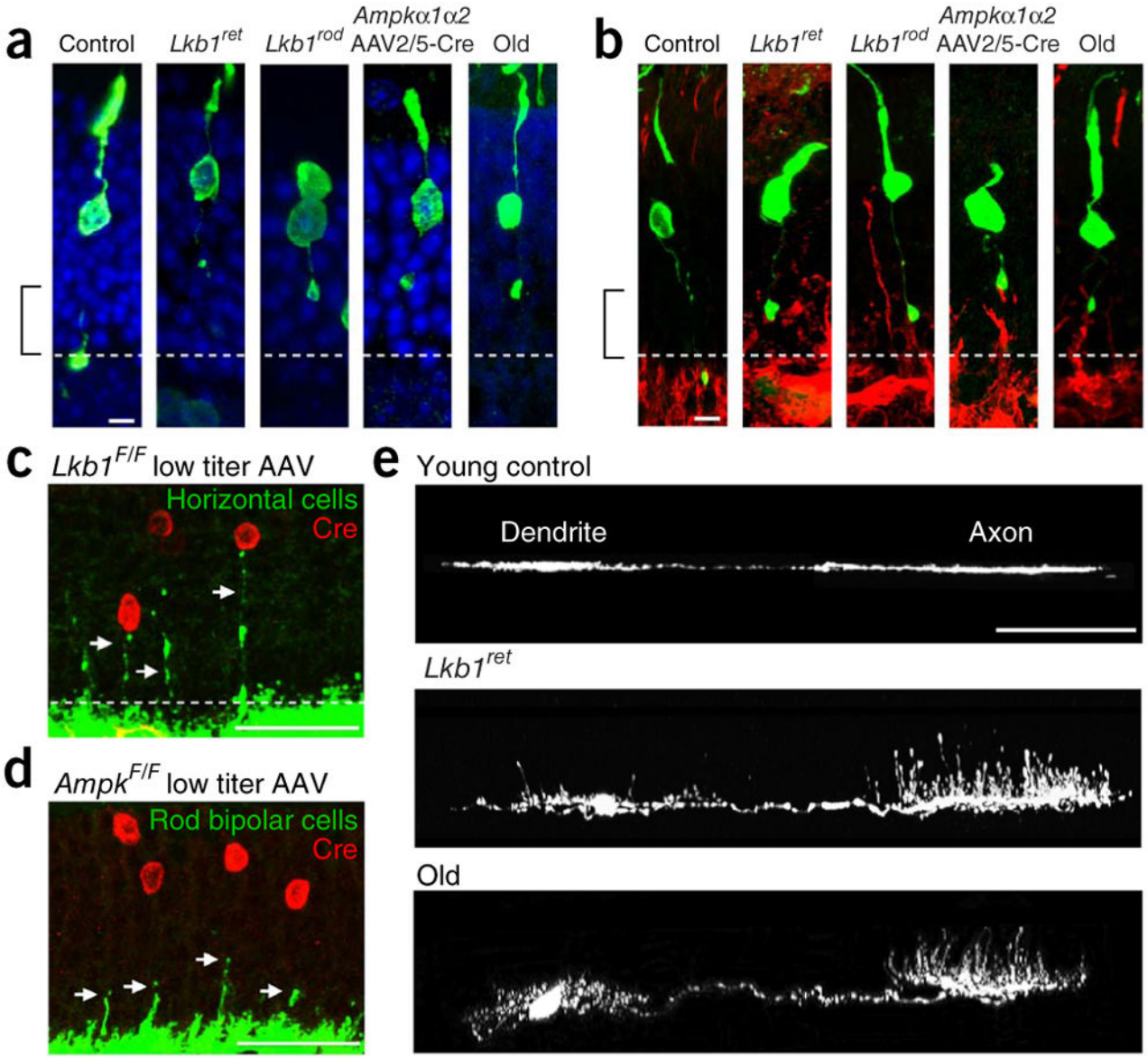

Figure 5.

Synaptic remodeling is accompanied by rod terminal retraction and postsynaptic sprouting. (**a**) Rod axons retracted in LKB1 mutants, *Ampkα1α2*/AAV2/5-Cre animals and old mice, as visualized by sparse infection with AAV2/5GFP. Scale bar represents 5 μm. Rods (GFP), green; nuclei, blue. (**b**) Retracted terminals were contacted by ectopic rod bipolar cell sprouts. Scale bar represents 5 μm. Rods (GFP), green; rod bipolar cells (PKCα), red. (**c**,**d**) Sparse *Lkb1* (**c**) or *Ampkα1α2* (**d**) deletion in adult retina using AAV-Cre induced single horizontal and rod bipolar cell sprouts directly beneath deficient neurons (arrows). Scale bars represent 25 μm. (**e**) Horizontal cell axons, but not dendrites, markedly remodeled in old and LKB1 mutant mice. Scale bar represents 50 μm. 4–8 animals were examined for each group. Dashed lines indicate the OPL/ONL border.

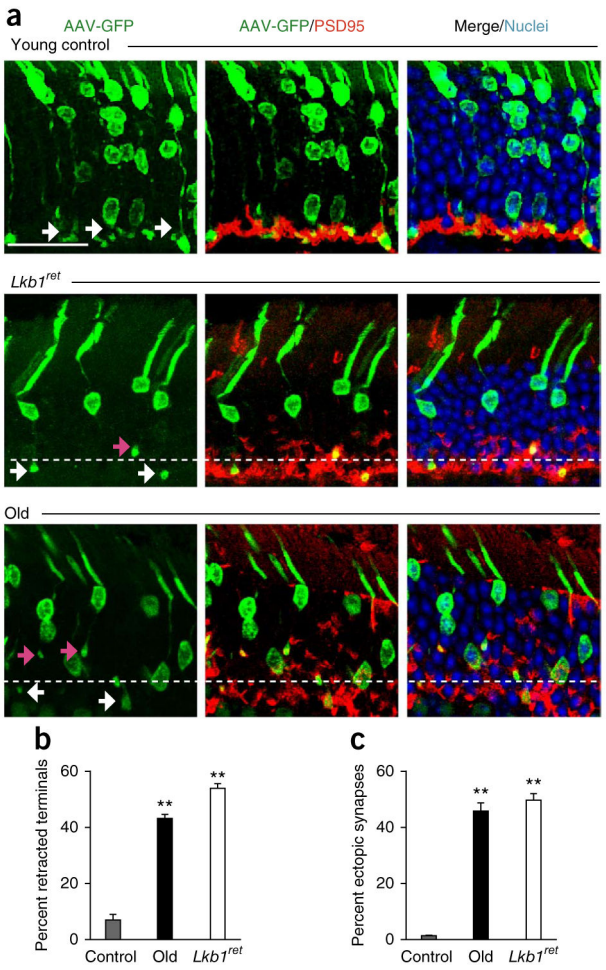

Figure 6.

Rods drive outer retina synaptic remodeling. (**a**) Rod terminals retracted frequently in *Lkb1*^{ret} and old mice, as visualized by infection with AAV2/5 GFP and co-staining with the rod terminal marker PSD95. Rods (GFP), PSD95, red; nuclei, blue. Scale bar represents 25 μm. White arrows indicate terminals in the OPL; magenta arrows indicate terminals above the OPL. Dashed lines indicate the OPL/ONL border. (**b**,**c**) The levels of rod retraction and ectopic synapse formation were similar. The percentage of retracted terminals (**b**) was quantified on the basis of single neuron terminal morphology (GFP), PSD95 and nuclei co-staining, whereas the percentage of ectopic synapses (**c**) was quantified following staining with Bassoon. Data are presented as mean ± s.e.m. of 31, 65 and 52 (**b**) and 23, 46 and 53 (**c**) measurements from 3 young control, old and *Lkb1*^{ret} mice, respectively. Data were evaluated using an unpaired, two-tailed Student's *t* test. $^{**}P < 0.0001$.

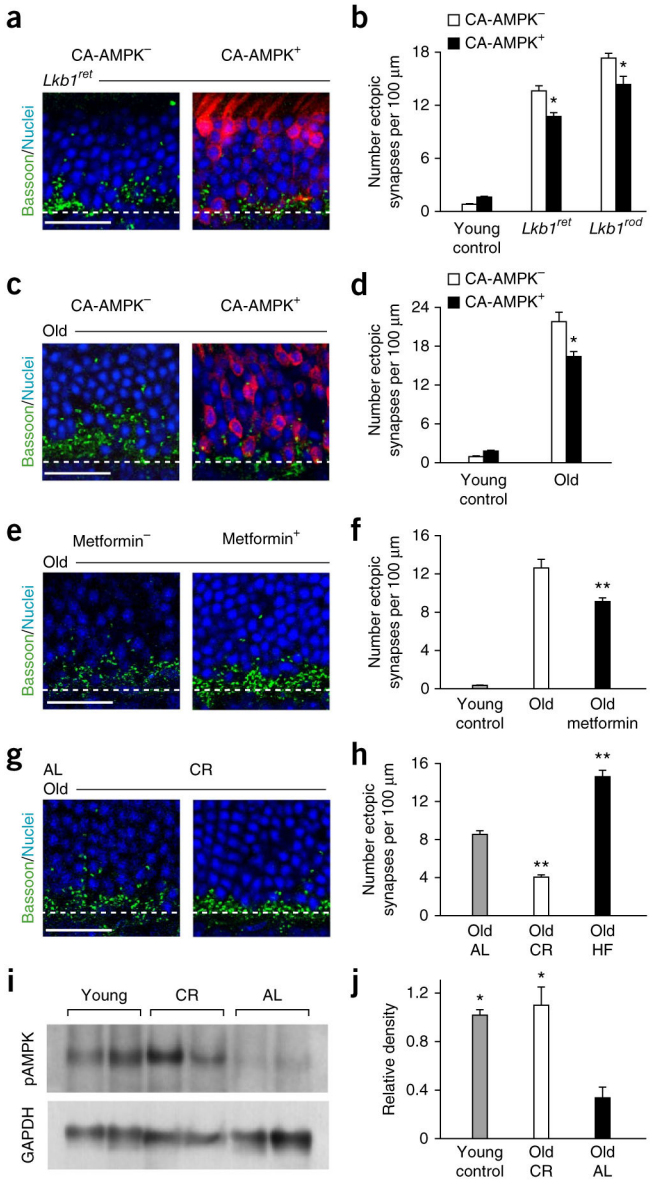

Figure 7.

Therapeutic attenuation of age-related synaptic changes. (**a**–**d**) CA-AMPK reversed synaptic remodeling. Adult LKB1 mutants (**a**,**b**) and old (24 months) wild-type mice (**c**,**d**) were infected with both AAV2/5 CA-AMPK and AAV2/5 GFP (as a tracer, red). Ectopic synapses were quantified 2 months later. Data are presented as mean ± s.e.m. of 153, 164 and 191 measurements from 5 young control, *Lkb1*^{ret} and *Lkb1*^{rod} animals, respectively (**b**, $P = 0.002$ for *Lkb1*^{ret} and $P = 0.004$ for *Lkb1*^{rod}); and 46 and 34 fields from 3 young and old animals, respectively (**d**, $P = 0.002$). (**e**,**f**) The number of ectopic synapses was quantified in control untreated and metformin-treated old animals. Data are presented as mean ± s.e.m. of 223, 66 and 198 fields from 4, 3 and 4 young, old untreated and old metformin-treated animals per group, respectively (**f**, $P < 0.0001$). (**g**,**h**) Mice were either calorically restricted (CR) or fed a high-fat (HF) diet. Data are presented as mean ± s.e.m. of 156, 132 and 55

fields from 6, 8 and 3 young, old CR and old *ad libitum* (AL) animals per group, respectively (**h**, $P < 0.0001$). Scale bars represent 25 μm in **a**, **c**, **e** and **g**. (**i**,**j**) Retina from young wild-type (WT) and old (24M) AL and CR controls were examined by immunoblot for the levels of activated AMPK (pAMPK, **i**). Caloric restriction significantly increased AMPK activation relative to old AL animals. Data are presented as mean ± s.e.m. from 6 animals per group (**j**, $P = 0.0002$ for young control and $P = 0.0003$ for old CR versus old AL). Full-length blots are presented in Supplementary Figure 11. Dashed lines indicate the OPL/ONL border. Data were evaluated using an unpaired, two-tailed Student's *t* test. $*P \leq 0.01$, $**P < 0.0001$.

Table 1

Full-field ERG amplitudes in control and *Lkb1*^{ret} mice

	Control mice, *n* = 6 mean ± s.e.m. (geometric mean)	**LKB1 mutants, *n* = 8* mean ± s.e.m. (geometric mean)**	***P* value†**
Rod A-wave ($\log_e$ μV)	5.18 ± 0.15 (178 μV)	4.52 ± 0.07 (92 μV)	0.0044
Rod B-wave ($\log_e$ μV)	6.35 ± 0.11 (572 μV)	5.42 ± 0.10 (226 μV)	<0.0001
Cone B-wave ($\log_e$ μV)	3.86 ± 0.09 (47 μV)	2.85 ± 0.11 (17 μV)	<0.0001

*Combined data from equal numbers of *Lkb1*$^{F/F}$ × *Chx10-Cre* and *LKB1*$^{F/F}$ × *Six3-Cre* mice.

†Calculated for the difference in means by repeated-measures regression with the eye as the unit of analysis using PROC MIXED of SAS allowing for unequal variances.